

Provided for non-commercial research and education use.
Not for reproduction, distribution or commercial use.



This article appeared in a journal published by Elsevier. The attached copy is furnished to the author for internal non-commercial research and education use, including for instruction at the authors institution and sharing with colleagues.

Other uses, including reproduction and distribution, or selling or licensing copies, or posting to personal, institutional or third party websites are prohibited.

In most cases authors are permitted to post their version of the article (e.g. in Word or Tex form) to their personal website or institutional repository. Authors requiring further information regarding Elsevier's archiving and manuscript policies are encouraged to visit:

<http://www.elsevier.com/authorsrights>



Hydroxyapatite coatings electrodeposited at near-physiological conditions

N. Metoki^a, L. Leifenberg-Kuznits^a, W. Kopelovich^a, L. Burstein^b, M. Gozin^c, N. Eliaz^{a,*}

^a Biomaterials and Corrosion Lab, Department of Materials Science and Engineering, Tel Aviv University, Ramat Aviv 6997801, Israel

^b Wolfson Applied Materials Research Center, Tel Aviv University, Ramat Aviv 6997801, Israel

^c School of Chemistry, Tel Aviv University, Ramat Aviv 6997801, Israel

ARTICLE INFO

Article history:

Received 10 June 2013

Accepted 24 December 2013

Available online 31 December 2013

Keywords:

Bioceramics

Hydroxyapatite

Thin films

Electrodeposition

Near-physiological conditions

ABSTRACT

Calcium phosphate (CaP) ceramics are used in orthopedics and dentistry due to their excellent biocompatibility and osseointegration. Plasma spraying has been the most common process for application of hydroxyapatite (HAp) coatings. Although electrodeposition (ED) has many potential advantages, very little has been published on ED of HAp at near-physiological conditions. Here we report the ED of uniform HAp–OCP (octacalcium phosphate) coatings on Ti–6Al–4V substrate at 37 °C, pH=7.4, following surface pretreatment. Thermodynamic calculations were first used to predict which CaP phases may precipitate from solution under different experimental conditions. Microscopic observation revealed that the coating formed in this study is similar to that formed by chemical deposition, and better mimics the biological apatites in terms of structure and phase content than coatings currently used in orthopedics.

© 2013 Elsevier B.V. All rights reserved.

1. Introduction

Calcium phosphate (CaP) bioceramics, especially hydroxyapatite (HAp, $\text{Ca}_5(\text{PO}_4)_3(\text{OH})$), have received much attention and have been clinically applied on orthopedic and dental implants due to their excellent biocompatibility and osseointegration. Various methods for applying CaP coatings have been reported in the literature, e.g. plasma spraying (PS), sputtering, sol–gel, chemical, etc. [1–5]. Currently, the most common method for applying such coatings on metallic substrates is PS [4]. However, great interest has evolved in recent years in electrochemical deposition (ED) due to its inherent advantages [5–15].

There is great interest in deposition of HAp and some other FDA-approved CaP phases such as octacalcium phosphate {OCP, $\text{Ca}_4(\text{HPO}_4)(\text{PO}_4)_2 \cdot 2.5\text{H}_2\text{O}$ } at near-physiological conditions (in terms of both temperature and pH) and low applied current density or potential. If successful, such a process may allow incorporation of ingredients such as collagens, growth factors, peptides, bone-forming cells, and enzymes on one hand, and antibiotics on the other hand.

Nevertheless, most of the published procedures for ED of CaP (see, for example, Refs. [5–22] and Table 1) have involved relatively high deposition temperatures (aiming at improving the uniformity of the coating and the bonding between the coating and the

substrate), high current densities, or non-physiological pH. For example, Kuo and Yen [18] demonstrated the formation of a uniform HAp coating on pure Ti substrate when using current densities higher than 10 mA/cm². At lower current densities (1–5 mA/cm²), dibasic calcium phosphate dihydrate (DCPD, or brushite, $\text{CaHPO}_4 \cdot 2\text{H}_2\text{O}$) was formed. Lopez-Heredia et al. [16] evaluated coatings that were formed at pH=7.4 within a wide range of temperatures and current densities, including at near-physiological conditions. High temperatures were found necessary to obtain thick and uniform coatings. Rößler et al. [20] revealed growth of channels of CaP upon which spheres of amorphous calcium phosphate (ACP) formed under near-physiological conditions. ACP is a well-known precursor to HAp [11].

Neither of these past studies demonstrated good coatings formed under conditions suitable for incorporation of biological matter and drugs (namely, physiological temperature and pH combined with very low current densities). In this paper we report a one-step electrodeposition of uniform, well adhered HAp–OCP coatings on Ti–6Al–4V alloy at $T=37$ °C, pH=7.4, and low current densities (below 0.1 mA/cm²).

2. Materials and methods

A geochemical computer program (PHREEQC) was first used to determine the tendency of different CaP phases to precipitate from solution under different conditions of bath composition, pH and temperature. The principles and use of such thermodynamic

* Corresponding author. Tel.: +972 3 640 7384; fax: +972 3 640 6648.
E-mail address: neliaz@eng.tau.ac.il (N. Eliaz).

Table 1
Operating conditions previously reported for electrodeposition of CaP.

T (°C)	pH	Applied current density or potential	Comment	References
60–95	4.2 or 6.0	–1.4 or –1.29 V vs. SCE	$i < 0.34 \text{ mA/cm}^2$. Best coatings obtained above 70 °C	[5–15]
25–80	7.4	8–120 mA/cm ²	Thickest and most uniform CaP obtained at high T and low i	[16]
90–200	7.2	5–25 mA/cm ²		[17]
25	4.11	1–20 mA/cm ²	Below 10 mA/cm ² , brushite (DCPD) was the main component	[18]
0–60	3.0	4–10 V	Deposited at 80 Torr. HAp formed at $E \geq 7 \text{ V}$, and its amount increased at 60 °C.	[19]
36	6.4	0.5–10 mA/cm ²	HAp was always accompanied by DCPD or amorphous calcium phosphate (ACP)	
60	7.4	–1.5 to –2.5 V vs. SCE	Very thin coatings (on the nanometer scale)	[20]
			Required subsequent immersion in simulated body fluid in order to form apatite	[22]

calculations have been demonstrated before [9]. The simulation results were subsequently verified experimentally.

A Ti–6Al–4V ELI grade rod was used as the substrate (working electrode). A series of surface pretreatments included mechanical grinding, surface activation in HF/HNO₃ solution, grit blasting (GB), and soaking in 5 M NaOH at 60 °C for 24 h. Electrodeposition was carried out in a standard three-electrode cell in which two graphite rods were used as counter electrodes and a saturated calomel electrode (SCE) was used as the reference electrode. The electrolyte consisted of Ca(NO₃)₂ and (NH₄)₂H₂PO₄. The solubility phase diagram of CaP was used as a starting point. Deposition conditions included pH=7.4, $T=37 \pm 0.1 \text{ °C}$, stirring at 200 rpm, applied potential of –1.4 V vs. SCE, and 2 h deposition time. The associated current density was fairly low, $\sim 0.1 \text{ mA/cm}^2$. More experimental details are provided elsewhere [6,7,12].

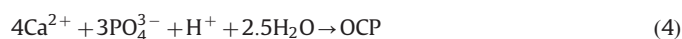
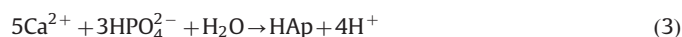
The surface morphology and the thickness of the coatings were characterized by environmental scanning electron microscopy (ESEM). X-ray diffraction (XRD) was used to determine the phase content. High-resolution X-ray photoelectron spectroscopy (XPS) measurements and analysis of the integrated intensities of the oxygen shake-up peaks were performed in accordance with the procedure described elsewhere in detail [11,12,22]. As analysis of the carbon C(1s) structure revealed that some carbonate was absorbed in the coating, the O/Ca, Ca/P, and O(1s)/O(1s) ratios were adjusted for carbonate [22]. The calculation took into account that the coating was formed on a substrate with an oxygen-containing surface layer. The strength of adhesion of the HAp coating to the metal substrate was measured by a tension test, as described elsewhere in detail [15].

3. Results and discussion

Fig. 1 shows the pH dependence of the saturation indices (SI) of HAp, OCP, DCPD, monetite (DCPA, CaHPO₄), and tricalcium phosphate {TCP, Ca₃(PO₄)₂}, with respect to three bath compositions: (i) “Nominal”, 610 μM Ca(NO₃)₂+360 μM (NH₄)₂H₂PO₄; (ii) “X0.1”, 61 μM Ca(NO₃)₂+36 μM (NH₄)₂H₂PO₄; and (iii) “X10”, 6100 μM Ca(NO₃)₂+3600 μM (NH₄)₂H₂PO₄. According to Fig. 1, for all three baths the solution is most supersaturated with respect to HAp throughout the whole pH range. The extent of supersaturation increases as the pH is raised. HAp is thus expected to precipitate spontaneously from solution over the whole pH range in all three cases. TCP may also precipitate from solution within most of the pH range. As the bath becomes more concentrated, it's possible precipitation extends to lower pH values (from 5.8 in Fig. 1a to 3.6 in Fig. 1c). At sufficiently high pH values, OCP may also form. The minimum pH value decreases from 9.2 in Fig. 1a to 5.4 in Fig. 1c. Although the initial pH in our experiments is 7.4, it is expected to rise in vicinity of the cathode during deposition [10], hence OCP may precipitate even from solution X0.1. Moreover, the samples were soaked in NaOH before electrodeposition. This pretreatment has been found to increase the pH in vicinity of the

cathode during electrodeposition [12]. Based on Fig. 1, DCPA and DCPD will not form in solutions X0.1 and Nominal, no matter the pH is, and will have a very small driving force for precipitation in solution X10 within the pH range 5.2–10.

In order to better understand the role of different species in deposition at pH 7.4 and $T=37 \text{ °C}$ versus deposition at pH 6.0 and $T=90 \text{ °C}$ [9], Table 2 lists the activities of the different species in the Nominal solution. The activities of PO_4^{3-} , HPO_4^{2-} , CaPO_4^- , and $\text{CaH}_2\text{PO}_4^+$ are higher in the former case, while those of OH^- , CaHPO_4 , and CaOH^+ are lower. The effect of temperature is different from that of pH at a constant temperature of 90 °C, where increased pH resulted in increase in the activities of PO_4^{3-} , OH^- , CaPO_4^- , and CaOH^+ , and a decrease in the activity of $\text{CaH}_2\text{PO}_4^+$. The main reactions for precipitation from solution of HAp and OCP are listed in Eqs. (1)–(5). From these equations it is evident that due to the aforementioned changes in the activities of different species, the likelihood of OCP formation is increased as the temperature is decreased from 90 °C to 37 °C while keeping the pH at 7.4.



Microscopic observation at low magnification revealed the coating that had been formed. As the coatings formed in solutions X0.1 and X10 were very thin, the focus here is on results for the Nominal solution only. Fig. 1(d and e) shows the typical surface morphology as evident by ESEM. The coating is fairly uniform and contains “mud-cracks”. Similar mud-cracks have been observed in carbonate apatite formed by sonoelectrodeposition, and were attributed to dehydration [23]. In our case, mud-cracks form already during the chemical pretreatment in NaOH [13]. Fig. 1(d and e) reveals the subsurface morphology of the coating. The surface morphology evident in Fig. 1(d and e) is significantly different from that of CaP electrodeposits formed before by Eliaz et al. at higher temperatures [7–10,12–14].

Metallurgical cross-sections (for example, see Fig. 2) revealed that the coating was $4.9 \pm 2.4 \text{ μm}$ thick ($n=16$). Interestingly, the deposition rate is similar to that measured by Wang et al. [7] for a CaP coating electrodeposited from the Nominal bath composition at $T=85 \text{ °C}$ and pH=6.0. The effect of bath temperature on the electrodeposition of CaPs has been discussed by Eliaz et al. for other pH values [9,10]. It was found that the thickness of the coating increases as the bath temperature is increased. In general, the dissociation constants of phosphoric acid, the density and dielectric constant of water, the A constant in the Debye–Hückel equation, the solubility products and the saturation indices of

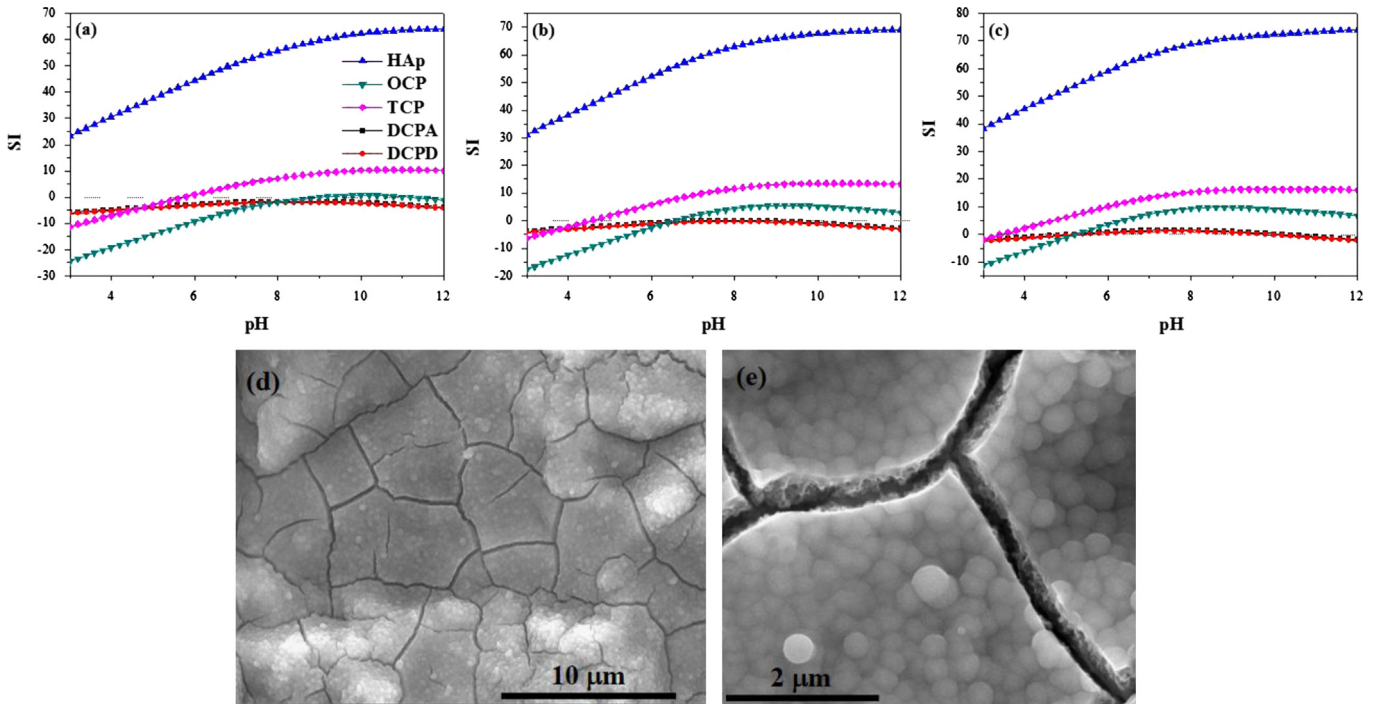


Fig. 1. The dependence of the saturation indices (SI) of five different calcium phosphates in various baths at 37 °C: (a) X0.1, (b) X10, and (c) Nominal. (d and e) ESEM images reveal the surface morphology of the CaP coating formed under near-physiological conditions in the Nominal solution.

Table 2

The activities (in Molal units) of species in the Nominal solution at different temperatures and pH values (PHREEQC calculation).

T(°C)	pH	Ca ²⁺	PO ₄ ³⁻	OH ⁻	HPO ₄ ²⁻	CaHPO ₄	CaPO ₄ ⁻	CaOH ⁺	CaH ₂ PO ₄ ⁺
90	6.0	4.33E-4	1.10E-11	3.92E-7	1.16E-5	1.16E-4	1.38E-8	3.39E-9	4.39E-8
90	7.4	2.96E-4	1.01E-9	9.84E-6	4.22E-5	2.88E-4	8.63E-7	5.83E-8	4.36E-9
37	7.4	4.82E-4	6.50E-9	5.97E-7	2.14E-4	3.01E-5	5.86E-6	5.75E-9	3.61E-7

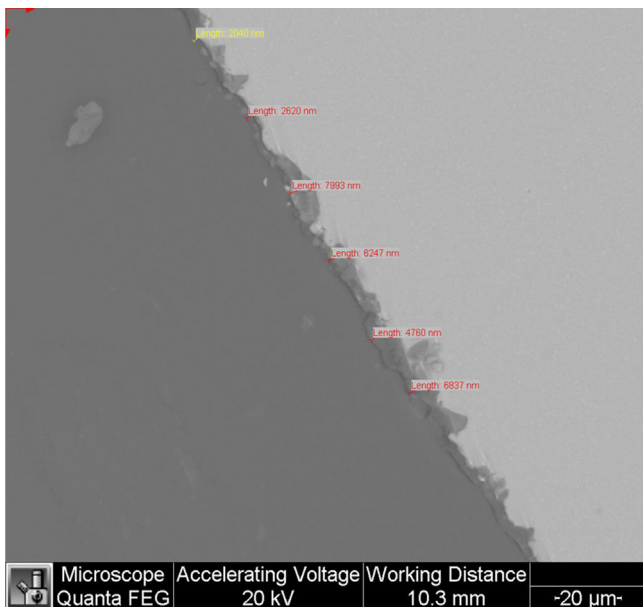


Fig. 2. SEM backscatter electrons image of a metallurgical cross-section. The thickness of the HAp coating in this field of view is $5.1 \pm 2.4 \mu\text{m}$.

different calcium phosphates are all temperature dependent. In addition, the OCP content increased as the bath pH was lowered from 6.0 to 4.2. The trends in the present study are opposite, indicating on a synergistic effect of bath temperature and pH. The

findings aforementioned imply that the mechanism of deposition must be different at $T=37\text{ °C}$ and $\text{pH}=7.4$ versus $T=85\text{ °C}$ and $\text{pH}=6.0$, as the different surface morphologies indicate.

XRD patterns (Fig. 3) revealed Ti reflections from the substrate along with HAp and OCP reflections. Energy dispersive spectroscopy (EDS) revealed a Ca/P atomic ratio of 1.85 ± 0.17 , when excluding all other elements from the analysis. However, Eliaz et al. [11] have shown that EDS analysis is not reliable in identification of CaP phases, while advanced XPS analysis is effective.

Indeed, advanced XPS measurements indicated that the coating consisted of 57% OCP and 43% HAp. The chemical composition of the coating is presented in Table 3. OCP is one of three phases that have been claimed to serve as precursors to the formation of HAp in vivo [11]. Furthermore, its presence in electrodeposited coatings and the related increase in the solubility of the coatings in vivo have been found to result in enhanced osseointegration [12]. The incorporation of OCP in the coating is likely to be beneficial in applications of controlled release of either antibiotics or incorporated biologic matter. Ti, Al and V from the substrate were not detected by XPS in this study, indicating that the coating is sufficiently thick.

The strength of adhesion of the coating to the metal substrate is one of the key factors determining the success or failure of the coating in vivo. International standards require that the value of the adhesion strength be at least 15 MPa [24,25]. The tensile stress to failure of the coating deposited in this study was $19.7 \pm 3.9\text{ MPa}$ ($n=5$). SEM-EDS analysis was used to determine the locus of failure; a cohesive failure (i.e. within the coating) was observed.

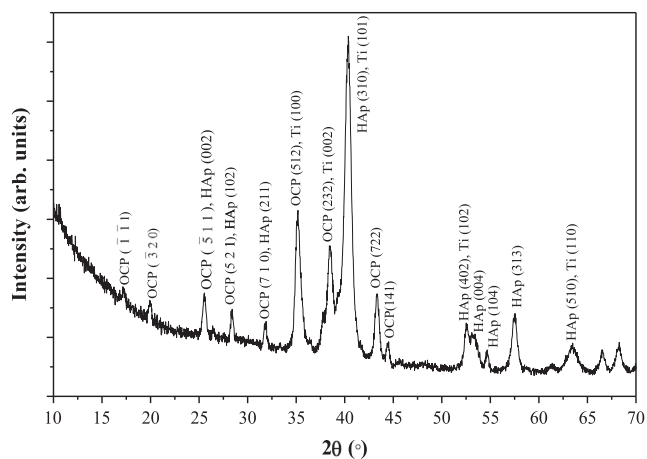


Fig. 3. XRD pattern showing that the coating formed under near-physiological conditions consists of HAp and OCP.

Table 3

Chemical composition (at%) and adjusted atom ratios and oxygen shake-up peak ratio, as determined by XPS.

O	Ca	P	C	Ca/P	O/Ca	O(1s) _{II} /O(1s)
51.03	15.50	11.79	21.69	1.27	3.25	0.067

Thus, the coating deposited in this study meets the requirement of the FDA in terms of adhesion strength.

4. Conclusions

In this work, a well adhered, homogenous coating consisted of HAp and OCP was deposited electrochemically on Ti–6Al–4V ELI rods at near-physiological conditions ($T=37\text{ }^{\circ}\text{C}$, $\text{pH}=7.4$). Thermodynamic calculations predicted the formation of HAp and OCP under these conditions. XRD and XPS analyses supported this prediction experimentally. While the surface morphology of the coating and the activities of different species in solution were found different from those of coatings electrodeposited at higher temperatures and lower pH values, the deposition rate was found similar, thus indicating that the mechanism of deposition may be different. The new coating may be loaded with both biological matter and antibiotics in order to further improve the osseointegration and infection resistance of future implants.

Acknowledgments

We thank Z. Barkay and Y. Rosenberg from the Wolfson Applied Materials Research Centre at Tel-Aviv University for their SEM and XRD characterization service, respectively.

References

[1] Kokubo T, Yamaguchi S. Bioactive metals prepared by surface modification: preparation and properties. In: Eliaz N, editor. Applications of electrochemistry

and nanotechnology in biology and medicine I. New York: Springer; 2011. p. 377–421.

[2] Guslitzer-Okner R, Mandler D. Electrochemical coating of medical implants. In: Eliaz N, editor. Applications of electrochemistry and nanotechnology in biology and medicine I. New York: Springer; 2011. p. 291–342.

[3] Gremillard L, Meille S, Chevalier J, Zhao J, Fridrici V, Kapsa Ph, et al. Degradation of bioceramics. In: Eliaz N, editor. Degradation of implant materials. New York: Springer; 2012. p. 195–252.

[4] Sun L, Berndt CC, Gross KA, Kucuk A. Material fundamentals and clinical performance of plasma-sprayed hydroxyapatite coating: a review. *J Biomed Mater Res B* 2001;58:570–92.

[5] Sridhar TM, Eliaz N, Mudali UK, Raj B. Electrophoretic deposition of hydroxyapatite coatings and corrosion aspects of metallic implants. *Corros Rev* 2002;20:255–93.

[6] Eliaz N, Sridhar TM, Mudali UK, Raj B. Electrochemical and electrophoretic deposition of hydroxyapatite for orthopaedic applications. *Surf Eng* 2005;21:238–42.

[7] Wang H, Eliaz N, Xiang Z, Hsu HP, Spector M, Hobbs LW. Early bone apposition in vivo on plasma-sprayed and electrochemically deposited hydroxyapatite coatings on titanium alloy. *Biomaterials* 2006;27:4192–203.

[8] Eliaz N, Eliyahu M. Electrochemical processes of nucleation and growth of hydroxyapatite on titanium supported by real-time electrochemical atomic force microscopy. *J Biomed Mater Res A* 2007;80:621–34.

[9] Eliaz N, Sridhar TM. Electrocrystallization of hydroxyapatite and its dependence on solution conditions. *Cryst Growth Des* 2008;8:3965–77.

[10] Eliaz N. Electrocrystallization of calcium phosphates. *Isr J Chem* 2008;48:159–68.

[11] Eliaz N, Kopelovitch W, Burstein L, Kobayashi E, Hanawa T. Electrochemical process of nucleation and growth of calcium phosphate on titanium supported by real-time quartz crystal microbalance measurements and X-ray photoelectron spectroscopy analysis. *J Biomed Mater Res A* 2009;89:270–80.

[12] Lakstein D, Kopelovitch W, Barkay Z, Bahaa M, Hendel D, Eliaz N. Enhanced osseointegration of grit-blasted, NaOH-treated and electrochemically hydroxyapatite-coated Ti–6Al–4V implants in rabbits. *Acta Biomater* 2009;5:2258–69.

[13] Eliaz N, Shmueli S, Shur I, Benayahu D, Aronov D, Rosenman G. The effect of surface treatment on the surface texture and contact angle of electrochemically deposited hydroxyapatite coating and on its interaction with bone-forming cells. *Acta Biomater* 2009;5:3178–91.

[14] Wang H, Eliaz N, Hobbs LW. The nanostructure of an electrochemically deposited hydroxyapatite coating. *Mater Lett* 2011;65:2455–7.

[15] Eliaz N, Ritman-Hertz O, Aronov D, Weinberg E, Shenhar Y, Rosenman G, et al. The effect of surface treatments on the adhesion of electrochemically deposited hydroxyapatite coating to titanium and on its interaction with cells and bacteria. *J Mater Sci Mater Med* 2011;22:1741–52.

[16] Lopez-Heredia MA, Weiss P, Layrolle P. An electrodeposition method of calcium phosphate coatings on titanium alloy. *J Mater Sci Mater Med* 2007;18:381–90.

[17] Ban S, Hasegawa J. Morphological regulation and crystal growth of hydrothermal-electrochemically deposited apatite. *Biomaterials* 2002;23:2965–72.

[18] Kuo MC, Yen SK. The process of electrochemical deposited hydroxyapatite coatings on biomedical titanium at room temperature. *Mater Sci Eng C* 2002;20:153–60.

[19] Wang SH, Shih WJ, Li WL, Hon MH, Wang MC. Morphology of the calcium phosphate coatings deposited on the Ti–6Al–4V substrate by an electrolytic method under 80 Torr. *J Eur Ceram Soc* 2005;25:3287–92.

[20] Rößler S, Sewing A, Stölzel M, Born R, Scharnweber D, Dard M, et al. Electrochemically assisted deposition of thin calcium phosphate coatings at near-physiological pH and temperature. *J Biomed Mater Res A* 2003;64:655–63.

[21] Park JH, Lee DY, Oh KT, Lee YK, Kim KM. Bioactivity of calcium phosphate coatings prepared by electrodeposition in a modified simulated body fluid. *Mater Lett* 2006;60:2573–7.

[22] Lu HB, Campbell CT, Graham DJ, Ratner BD. Surface characterization of hydroxyapatite and related calcium phosphates by XPS and TOF-SIMS. *Anal Chem* 2000;72:2886–94.

[23] Xiong X, Li H, Zeng X, Zou J, Tang H. Deposition kinetics of apatite coating on CVI carbon/carbon composite by sonoelectrodeposition technique. *Rare Met Mater Eng* 2006;35:1418–23.

[24] BS ISO 13779-2:2000. Implants for surgery—Hydroxyapatite—Part 2: coatings of hydroxyapatite. British Standards Institution, London, UK.

[25] Callahan TJ, Gantenberg JB, Sands BE. Calcium phosphate (Ca-P) coating draft guidance for preparation of Food and Drug Administration (FDA) submissions for orthopedic and dental endosseous implants. In: Horowitz E, Parr JE, editors. ASTMSTP 1196: characterization and performance of calcium phosphate coatings for implants. PA: ASTM; 1994. p. 185–97.